Rapidity dependence of Bose-Einstein correlations at SPS energies

S. Kniege [1], C. Alt[1], T. Anticic[2], B. Baatar[3], D. Barna[4], J. Bartke[5],
L. Betev[6], H. Bialkowska[7], C. Blume[1], B. Boimska[7], M. Botje[8],
J. Bracinik[9], R. Bramm[1], P. Bunčić[1,6], V. Cerny[9], P. Christakoglou[10],
O. Chvala[11], J.G. Cramer[12], P. Csató[4], P. Dinkelaker [1], V. Eckardt [13],
D. Flierl [1], Z. Fodor [4], P. Foka [14], V. Friese [14], J. Gál [4], M. Gaździcki [1,15],
V. Genchev[16], G. Georgopoulos[10], E. Gładysz [5], K. Grebieszkow [17],
S. Hegyi [4], C. Höhne [18], K. Kadija [2], A. Karev [13], M. Kliemant [1],
V.I. Kolesnikov [3], E. Kornas [5], R. Korus [15], M. Kowalski [5], I. Kraus [14],
M. Kreps [9], A. Laszlo [4], M. van Leeuwen [8], P. Lévai [4], L. Litov [19],
B. Lungwitz [1], M. Makariev [19], A.I. Malakhov [3], M. Mateev [19],
G.L. Melkumov [3], A. Mischke [14], M. Mitrovski [1], J. Molnár [4],
St. Mrówczyński[15], V. Nicolic[12], G. Pálla [4], A.D. Panagiotou[10],
D. Panayotov [19], A. Petridis [10], M. Pikna [9], D. Prindle [20], F. Pühlhofer[18],
R. Renfordt [1], C. Roland [21], G. Roland [21], M. Rybczyński[15], A. Rybicki [5,6],
A. Sandoval [14], N. Schmitz [13], T. Schuster [1], P. Seyboth [13], F. Siklér [4],
B. Sitar [9], E. Skrzypczak [17], G. Stefanek [15], R. Stock [1], C. Strabel [1],
H. Ströbele [1], T. Susa [2], I. Szentpétery[4], J. Sziklai [4], P. Szymanski [15,15],
V. Trubnikov [15], D. Varga [4], M. Vassiliou [10], G.I. Veres [4,21],
G. Vesztergombi [4], D. Vranić [14], A. Wetzler [1], Z. Włodarczyk[15] and
J. Zimányi [4]

[1]*Fachbereich Physik der Universität, Frankfurt, Germany.*
[2]*Rudjer Boskovic Institute, Zagreb, Croatia.*
[3]*Joint Institute for Nuclear Research, Dubna, Russia.*
[4]*KFKI Research Institute for Particle and Nuclear Physics,Budapest,Hungary.*
[5]*Institute of Nuclear Physics, Cracow, Poland.*
[6]*CERN, Geneva, Switzerland.*
[7]*Institute for Nuclear Studies, Warsaw, Poland.*
[8]*NIKHEF, Amsterdam, Netherlands.*
[9]*Comenius University, Bratislava, Slovakia.*
[10]*Department of Physics, University of Athens, Athens, Greece.*
[11]*Institute of Particle and Nuclear Physics, Charles University, Prague,Czech Republic.*
[12]*Nuclear Physics Laboratory, University of Washington, Seattle, WA, USA.*
[13]*Max-Planck-Institut für Physik, Munich, Germany.*
[14]*Gesellschaft für Schwerionenforschung (GSI), Darmstadt, Germany.*
[15]*Institute of Physics Świetokrzyska Academy, Kielce, Poland.*
[16]*Institute for Nuclear Research and Nuclear Energy,Sofia, Bulgaria.*
[17]*Institute for Experimental Physics, University of Warsaw, Warsaw,Poland.*
[18]*Fachbereich Physik der Universität, Marburg, Germany.*
[19]*Atomic Physics Department, Sofia University St. Kliment Ohridski, Sofia,Bulgaria.*
[20]*University of Houston, Houston, TX, USA.*

[21]*MIT, Cambridge, USA.*

Abstract. This article is devoted to results on π^--π^--Bose-Einstein correlations in central Pb+Pb collisions measured by the NA49 experiment at the CERN SPS. Rapidity as well as transverse momentum dependences of the correlation lengths will be shown for collisions at 20*A*, 30*A*, 40*A*, 80*A*, and 158*A* GeV beam energy. Only a weak energy dependence of the radii is observed at SPS energies. The k_t-dependence of the correlation lengths as well as the single particle m_t-spectra will be compared to model calculations. The rapidity dependence is analysed in a range of 2.5 units of rapidity starting at the center of mass rapidity at each beam energy. The correlation lengths measured in the longitudinally comoving system show only a weak dependence on rapidity.

1. INTRODUCTION

The measurement of correlations of identical bosons in heavy ion collisions provides a unique tool to investigate the space time evolution of the particle emitting source. Bose-Einstein correlations are observed as an enhancement of the yield of pairs of particles with small relative momenta. Measurements of the range and strength of the correlations in momentum space allow to derive the extension of the source in coordinate space. Due to space momentum correlations in expanding sources the correlations do not reflect the whole extensions of the source. In such a scenario, the study of the correlations in different regions of phase space helps to understand the evolution of the source. While the dependence of the correlation lengths on the mean transverse momentum $k_t = \frac{1}{2}|\vec{p}_{t,1} + \vec{p}_{t,2}|$ of the pairs reflects the transverse expansion dynamics of the source the dependence on the pair rapidity $Y = \frac{1}{2}\log\left(\frac{E_1+E_2+p_{z,1}+p_{z,2}}{E_1+E_2-p_{z,1}-p_{z,2}}\right)$, which is measured in the center of mass system, should shed light on the profile of the source in longitudinal direction. The large acceptance of the NA49 experiment allows us to obtain a comprehensive picture of the dynamical evolution of the source.

The article is organized as follows: A brief survey of the experiment, the construction of the correlation function and the fit method are presented in section 2. In section 3, crucial systematic uncertainties in the analysis due to detector effects are discussed. The results on the k_t- as well as the Y- dependence of the correlation lengths are presented in section 4 and compared to model calculations.

2. EXPERIMENTAL SETUP AND ANALYSIS

NA49 [1] is a fixed target experiment located at the CERN SPS comprising four large-volume Time Projection Chambers (TPC), two of which are located inside the magnetic field of two superconducting dipole magnets (Figure 1). The TPCs are read out at 90 (MTPC) and 72 (VTPC) pad rows resulting in a very good determination of the momentum of the traversing particles. A zero degree calorimeter at the downstream end of the experiment is used to trigger on the centrality of the collisions. The data presented here correspond to the 7.2% most central events for data samples taken at 20*A*, 30*A*, 40*A*,
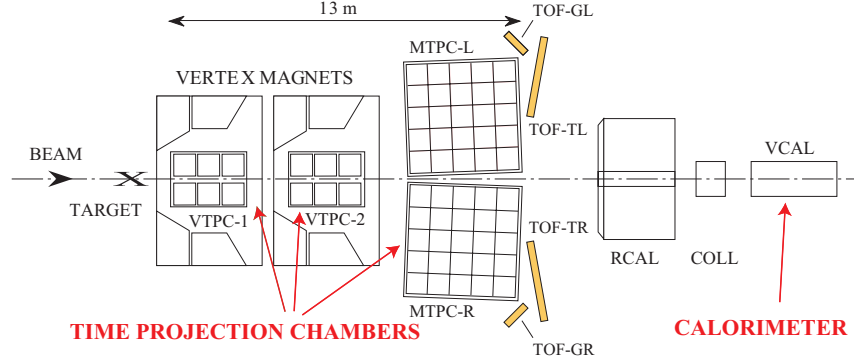
FIGURE 1. NA49 detector setup.

80A, and 158A GeV beam energy. By scaling the magnetic field it was possible to obtain a similar coverage of phase space relative to the center of mass rapidity for the different beam energies. Measuring the specific energy loss dE/dx of charged particles in the gas of the TPCs with a resolution of 3-4% allows particle identification. However, due to ambiguities in particle identification by specific energy loss measurements in certain regions of phase space, negative hadrons rather than identified negative pions are studied in this analysis.

The correlation function is constructed as the ratio of a distribution of the momentum difference of pairs from the same event (signal) and a mixed event background distribution (background). Following the approach of Pratt and Bertsch [2, 4] the momentum difference is decomposed into a component parallel to the beam axis q_{long} and two components in the transverse plane q_{out} and q_{side} with q_{out} defined parallel, and q_{side} perpendicular to k_t. The correlation function is parameterised by a Gaussian function

$$C_2(q)_{BP} = 1 + \lambda \cdot \exp(-R_{out}^2 q_{out}^2 - R_{side}^2 q_{side}^2 - R_{long}^2 q_{long}^2 - 2R_{outlong}^2 q_{out} q_{long}) \quad (1)$$

and the parameters R_{out}, R_{side}, R_{long}, $R_{outlong}$, and λ are determined by a fit to the measured correlation function. The Coulomb repulsion of the particles is accounted for by weighting the theoretical Bose-Einstein correlation function $C_2(q)_{BP}$ by a factor $F(q_{inv}, <r>)$ [3] in the fit procedure. The weight is determined by the invariant momentum difference q_{inv} of the pair and the mean pair separation $<r>$ of the particles in the source. According to [3] this quantity can be derived from the extracted radii. We therefore determine the source parameters as well as the value of $<r>$ in an iterative fit-procedure. For following fit function was used:

$$C_2(q)_f = n\{p \cdot (C_2(q)_{BP} \cdot F(q, <r>)) + (1-p)\}. \quad (2)$$

The contamination of the sample with pairs of non-identical particles and pairs of pions from long lived resonances or weak decays is accounted for by a purity factor p which is determined by a VENUS/GEANT simulation. The fit parameter n is introduced to account for the different statistics in signal and background distributions. Beside the uncertainties which arise due to the construction of the correlation function and the fit formalism there are further detector related effects which will be discussed in the next section.

3. SYSTEMATIC STUDIES

3.1. Two track resolution

The momentum difference of a pair is closely related to the distance of the tracks traversing the detector. Bose-Einstein correlations are restricted to a narrow window in momentum difference, hence it is crucial to understand the two track resolution of the detector. The overlap of charge clusters induced at the pad planes of the TPCs can lead to an assignment of points to the wrong track or in an extreme case to complete merging of two tracks. In this case, a pair with small relative momentum will be lost in the signal distribution and the observable Bose-Einstein enhancement will be reduced. To study the impact of the limited two track resolution on the extracted radii, the distance of the tracks was measured at each pad row where both tracks lie in the sensitive volume of the TPCs. Starting from the downstream end of the TPCs the distance of closest approach (dca) of two tracks after a given number of passed pad rows n_{rows} was determined. Pairs with a dca smaller than a given cut value dca_{cut} were rejected both from the signal and the background distribution. The impact of a variation of the two parameters dca_{cut} and n_{rows} on the correlation function is shown in Figure 2. Requiring only small values of dca_{cut} and n_{rows}, tracks can approach each other very closely over a considerable part of the track length in the TPCs. In this case, track merging effects can lead to a significant loss of pairs in the signal. This effect is very pronounced at high transverse momenta and shows up in an undershoot of the projection of the correlation function onto q_{out} (Figure 2a). Increasing the cut parameters, the influence of merging effects is reduced, the undershoot of the correlation function vanishes and the extracted radii vary only by less than 0.2 fm (Figure 2b). This can serve as an estimate of the systematic error on the radii due to the specific treatment of the two track inefficiencies in this analysis.

Further systematic errors on the radii arise due to uncertainties concerning the treatment of the Coulomb interaction (which can significantly influence the parameters R_{out} and λ), the missing particle identification, the finite momentum resolution of the detector and
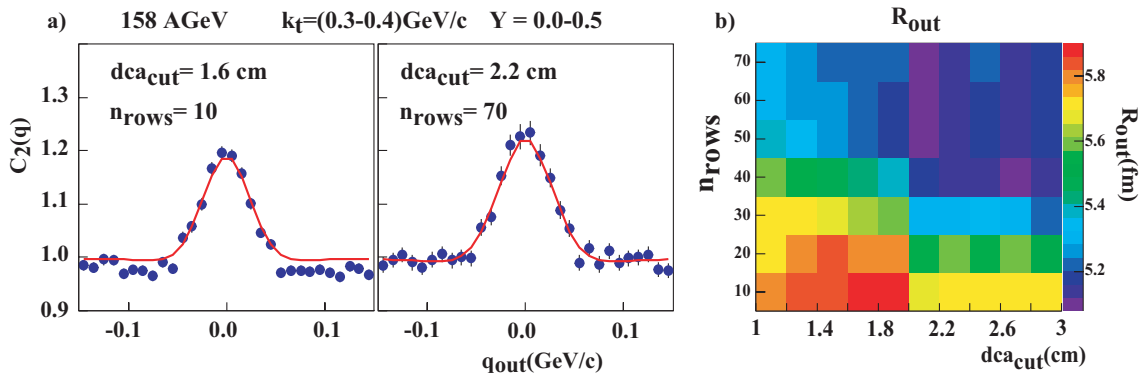

FIGURE 2. a) Impact of two track resolution inefficiencies on the shape of the correlation function and b) fit results for R_{out} for different combinations of the cut parameters dca_{cut} and n_{rows}.

the normalisation of the correlation function. The overall systematic error on the radii is not specified for each k_t-Y-bin but estimated to be smaller than 1 fm for all extracted radii.

4. RESULTS

4.1. The k_t-dependence

Figure 3 presents the k_t-dependence of the radii at midrapidity. Radius and λ parameters were obtained from fits of (2) to the correlation function in bins of Y and k_t. Since the influence of the finite momentum resolution was found to be small, no corrections were applied for this effect. The bin width in k_t was chosen to be 0.1 GeV/c and increased to 0.2 GeV/c for the last bin ((0.4-0.6) GeV/c) to obtain sufficient statistics at all energies. A strong decrease of R_{long} with k_t is observed. R_{out} is slightly larger than R_{side} for all energies indicating a finite duration of particle emission [4]. Also shown in this picture is a fit of the k_t-dependence of the radii according to a blast wave parameterisation [5] of the source. In this model the source is treated as boost invariant in the longitudinal direction. In the transverse direction a box-shaped density profile and a linearly increasing flow profile is assumed. Space momentum correlations induced by flow reduce the measured correlation lengths. This effect is partly compensated in case of a superimposed thermal velocity field. Therefore ambiguities arise in the two model parameters temperature and flow, which can not be resolved by only analysing the k_t-dependence of the radii. To resolve these ambiguities the single particle p_t-spectra of protons and negatively charged pions measured by NA49 were fitted to a parameterisation derived from the same model. The lines in Figure 3 correspond to a combined fit to the radii and the particle p_t-spectra. As expected from the weak energy dependence of the radii only small variations of the extracted source parameters were observed. The extracted parameters were the temperature T, the maximum transverse flow rapidity ρ, the transverse geometrical radius R, the emission time τ and the emission duration $\Delta\tau$. The fit results are inserted in Figure 3. The temperature T slightly increases with the beam energy, transverse flow and geometrical radius stay approximately constant over the observed energy range. For the emission time we obtain values of 5.4 to 6.8 fm/c. The fit slightly overpredicts R_{side} at high k_t but still results in a finite emission duration of 2.2-3.2 fm/c. The fit might be further constrained by adding more particle spectra or by including contributions from resonance decays in the model.

4.2. Y-dependence

The model described in section 4.1 is only applicable in case of a longitudinally boost invariant source. Under such conditions it is expected that the cross term $R_{outlong}$ vanishes [6]. Considering the systematic error of 1 fm this condition is fulfilled to good approximation at midrapidity. In Figure 4 the rapidity dependence of R_{long}, R_{side}, R_{out}, and $R_{outlong}$ is shown at k_t=(0.0-0.1) GeV/c for the different beam energies. In [7] the impact of a non-boost invariant expansion on the parameter $R_{outlong}$ is studied.
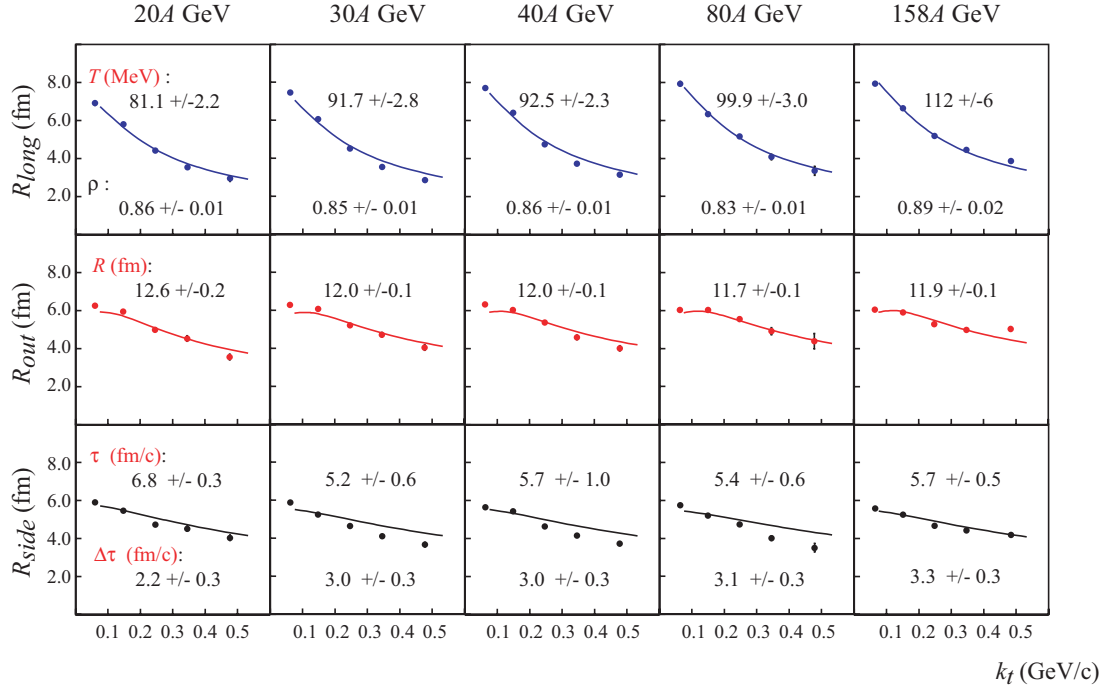
The figure contains a 3×5 grid of plots. Column headers (top): 20*A* GeV, 30*A* GeV, 40*A* GeV, 80*A* GeV, 158*A* GeV. Row labels (left axes): R_{long} (fm), R_{out} (fm), R_{side} (fm). The x-axis is k_t (GeV/c) with ticks 0.1 0.2 0.3 0.4 0.5.

Annotations in the R_{long} row:
T (MeV): 81.1 +/-2.2; 91.7 +/-2.8; 92.5 +/-2.3; 99.9 +/-3.0; 112 +/-6
ρ: 0.86 +/- 0.01; 0.85 +/- 0.01; 0.86 +/- 0.01; 0.83 +/- 0.01; 0.89 +/- 0.02

Annotations in the R_{out} row:
R (fm): 12.6 +/-0.2; 12.0 +/-0.1; 12.0 +/-0.1; 11.7 +/-0.1; 11.9 +/-0.1

Annotations in the R_{side} row:
τ (fm/c): 6.8 +/- 0.3; 5.2 +/- 0.6; 5.7 +/- 1.0; 5.4 +/- 0.6; 5.7 +/- 0.5
Δτ (fm/c): 2.2 +/- 0.3; 3.0 +/- 0.3; 3.0 +/- 0.3; 3.1 +/- 0.3; 3.3 +/- 0.3

FIGURE 3. The k_t-dependence of R_{side}, R_{out}, and R_{long} at midrapidity ($0.0 < Y < 0.5$) for the different data sets (dots). The lines correspond to a combined fit of the blast wave model to the radii and the single particle p_t-spectra.

An increase of $R_{outlong}$ with increasing rapidity is predicted due to the decrease of the inclusive pion yields and is in agreement with the results for all energies. However a change in the longitudinal expansion dynamics which is indicated by the change in $R_{outlong}$ is not reflected in the rapidity dependence of the other observables. R_{side}, which is supposed to determine the geometrical size of the source [8] does not change significantly with rapidity. R_{out} is approximately constant over the investigated rapidity region. Only slight changes in R_{long} are observed. These are even less pronounced at higher transverse momenta.

In summary, a distinct energy dependence of the radii is not observed even though there is a dramatic change in the energy dependence of other hadronic observables like e.g. the kaon to pion ratio [9]. Furthermore the radii do not show a pronounced rapidity dependence, in contrast to the particle yields which decrease strongly with rapidity.
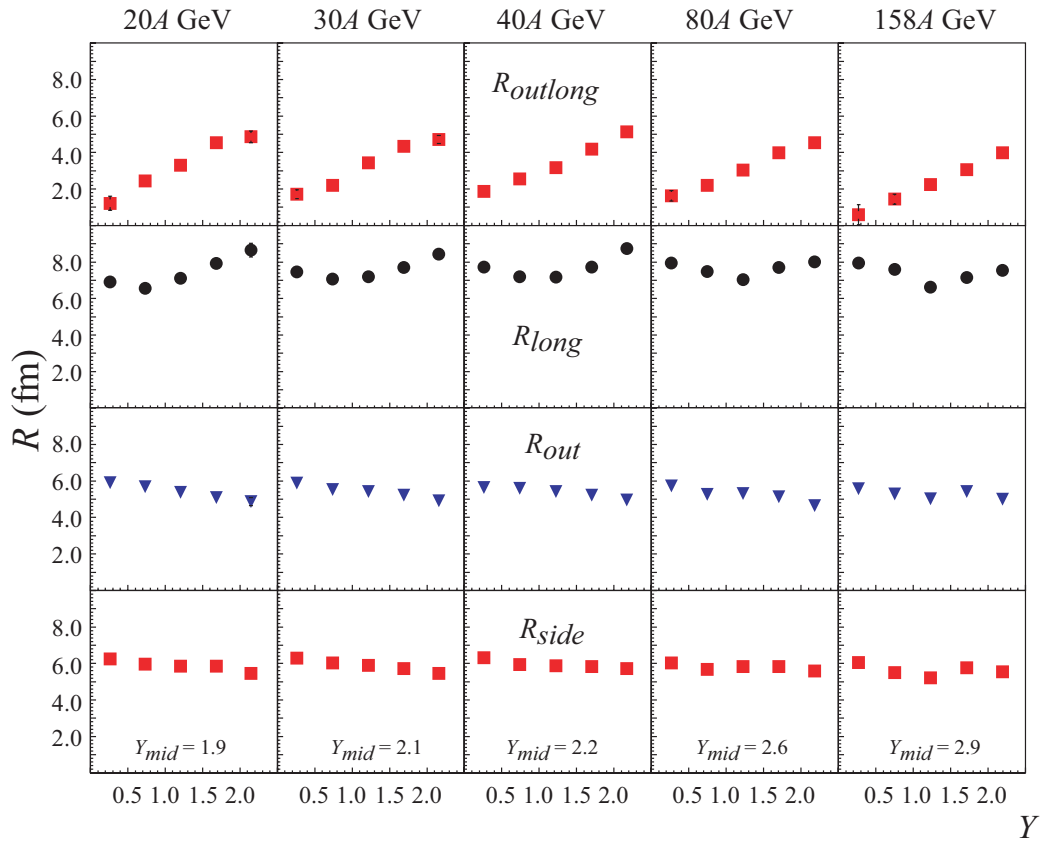
ACKNOWLEDGMENTS

FIGURE 4. Rapidity dependence of R_{side}, R_{out}, R_{long}, and $R_{outlong}$ at k_t=(0.0-0.1) GeV/c for the different beam energies. Shown are as well the midrapidity values Y_{mid} for the different beam energies.

REFERENCES

1. S. Afanasiev et al., NIM A430 (1999) 210-244
2. S. Pratt, Phys. Rev. **D 33** (1986) 1314-1327
3. Yu. M. Sinyukov et al., Phys. Lett. **B 432** (1998) 248-257
4. G. F. Bertsch, Nucl.Phys. **A 498** (1989) 173c-180c
5. F. Retriere, M. Lisa, Phys. Rev. **C 70** 044907 (2004)
6. S. Chapman, P. Scotto und U. Heinz, Phys.Rev.Lett **74** (1995) 4400-4403
7. S. Chapman, P. Scotto und U. Heinz, Nucl.Phys. **A 590** (1995) 449c-452c
8. S. Chapman, J. Nix and U. Heinz, Phys. Rev. **C 52** (1995) 2694-2703
9. M. Gazdzicki, J. Phys. G: Nucl. Part. Phys. **30** (2004) 701-708